Journal of Electroanalytical Chemistry 703 (2013) 14–22

Contents lists available at SciVerse ScienceDirect

Journal of Electroanalytical Chemistry

journal homepage: www.elsevier.com/locate/jelechem

Fluorinated models of the iron-only hydrogenase: An electrochemical study of the influence of an electron-withdrawing bridge on the proton reduction overpotential and catalyst stability ☆

Faith Ridley, Shishir Ghosh, Graeme Hogarth *, Nathan Hollingsworth, Katherine B. Holt *, David G. Unwin

Department of Chemistry, University College London, 20 Gordon Street, London WC1H 0AJ, UK

ARTICLE INFO

Article history:
Received 27 March 2013
Received in revised form 14 May 2013
Accepted 21 May 2013
Available online 31 May 2013

Keywords:
Electrocatalysis
Di-iron complexes
Proton reduction
Hydrogenases
Phosphines
Fluorinated thiolate

ABSTRACT

Here we report the synthesis, electrochemistry and electrocatalytic activity of $Fe_2(CO)_6(\mu\text{-}SC_6F_5)_2$ (**1**) where the highly fluorinated bridge is electron-withdrawing, resulting in decreased electron-density at the iron–iron bond. Additionally we discuss the related substituted complexes $Fe_2(CO)_5(PPh_3)(\mu\text{-}SC_6F_5)_2$ (**2**) and $Fe_2(CO)_4(\mu\text{-}Ph_2PCH_2PPh_2)(\mu\text{-}SC_6F_5)_2$ (**3**). As none of the complexes could be protonated in their neutral form it was found that proton reduction catalysis in the presence of strong acid (HBF_4) took place at the potential of the first reduction of complex **1** and **3**, following an EC mechanism. Complex **2** was unstable in the presence of strong acid. For **1** the potential at which proton reduction took place represented a relatively mild reduction potential (−1.15 V vs. Fc/Fc^+ in acetonitrile) that was comparable to examples of similar complexes in the literature. Complex **1** generated a small concentration of a highly catalytic species after electrochemical reduction, which we attribute to cleavage of the Fe–Fe bond and formation of a mono-nuclear iron species or to Fe–S bond breakage generating a vacant coordination site. The contributions to the catalytic currents were simulated using DigiSim, where it was found that the rate limiting step for **3** was the elimination of H_2. It was also found that the highly catalytic species generated after reduction of **1** was more basic than $\mathbf{1}^-$ and also that protonation of this species was faster.

1. Introduction

[Fe–Fe] hydrogenase enzymes rapidly and reversibly reduce protons to form hydrogen with negligible overpotential in neutral pH solution conditions [1]. With hydrogen increasingly cited as a clean and renewable energy source, low energy routes to its generation attract considerable interest. Understanding how hydrogenase enzymes are able to generate hydrogen with such remarkable efficiency is an ongoing research effort, particularly using protein film voltammetry techniques [2]. An alternate approach is to study the electrocatalytic activity of model compounds mimicking the enzyme active site [3]. First efforts were concentrated on producing faithful structural models of the active site known as the 'H cluster', which is a dithiolate bridged diiron cluster, ligated with biologically unusual CO and CN^- (Chart 1a) [4]. Although chemists have risen to the synthetic challenge of producing almost exact structural models of the H-cluster [5] so far the performance of the mimic compounds, when studied as homogeneous proton reduction catalysts in non-aqueous solvents, has generally been disappointing. However very recently Dey and co-workers have achieved proton reduction catalysis in aqueous solution using an electrode-immobilised azadithiolate-bridged model with an onset potential of −0.36 V vs. NHE and with impressive Faradaic efficiency and turnover frequency [6].

Catalysis can take place either *via* initial reduction followed by protonation (an EC mechanism) or, if the complex has sufficient basicity, by protonation followed by electrochemical reduction (a CE mechanism). Hexacarbonyl complexes such as $Fe_2(CO)_6(\mu\text{-pdt})$ (Chart 1b) are not usually basic enough to be protonated except by acids derived from strong Lewis acids [7]. Therefore, for catalysis to take place the complex must first be reduced, resulting in increased electron-density at the iron–iron bond and subsequent protonation [8]. Catalysis therefore takes place at the potential of the first reduction of the complex, which usually represents a considerable overpotential from the ideal thermodynamic potential of proton reduction. The basicity of the complex can be increased by substitution with electron-donating ligands, such as cyanide [4] and phosphines [9], resulting in protonation across the iron–iron bond without prior reduction. Protonation of these basic complexes can be quite rapid, but in some cases is still rate-limiting

* Corresponding authors. Tel.: +44 0207 6791027 (K.B. Holt).
E-mail address: k.b.holt@ucl.ac.uk (K.B. Holt).

1572-6657/$ - see front matter © 2013 The Authors. Published by Elsevier B.V. All rights reserved.
http://dx.doi.org/10.1016/j.jelechem.2013.05.018

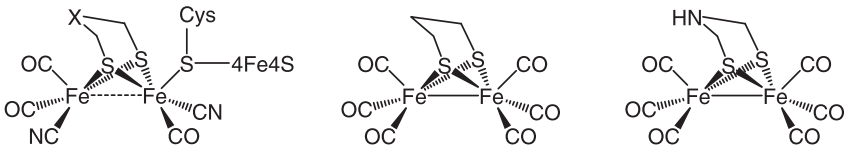

Chart 1. Left: Structure of H cluster (X now widely accepted as NH); Centre: structure of pdt hexacarbonyl; Right: structure of adt hexacarbonyl.

due to slow isomerisation processes [10]. The removal of electron-density from the bond by the proton allows reduction of the protonated complex to take place at 0.5–1 V more positive potential than the reduction of the non-protonated species. This CE mechanism could potentially result in lower overpotentials for catalysis, but unfortunately the increased electron-density provided by the ligands pushes the reduction potential of the complex more negative [11], so there is very little energetic gain from using this approach.

Researchers have addressed this issue by designing complexes with electron-withdrawing groups in the bridge. This results in less electron-density at the iron–iron bond, hence a less negative reduction potential [12–22]. Although the neutral complexes do not protonate at the iron centres and catalysis must take place by an EC mechanism, the potential at which this occurs is not prohibitively negative and represents an improved overpotential for proton reduction. One approach has been to introduce a basic N-containing moiety to the bridge that withdraws electron-density from the metal centres when it is protonated [12]. This approach may be considered biomimetic, as a similar mechanism may operate in the enzyme, where the dithiolate bridge is believed to be azadithiolate (adt) rather than propanedithiolate (pdt) (Chart 1c).

Other researchers have introduced more exotic bridges in an attempt to produce complexes with less negative reduction potentials [13–22]. From the perspective of reduction potential the most successful in literature to date is the *o*-carborane (1,2,-*clos*-*o*-$C_2B_{10}H_{12}$) cluster bridged complex synthesised by Ott et al. [13], which undergoes reduction at $E_{1/2} = -0.88$ V vs. Fc/Fc^+ in MeCN and protonation and further reduction at the same potential in the presence of a strong acid. Other electron-withdrawing moieties have been introduced at the bridge, including benzenedithiolate (bdt) [14–16] and related chlorine-substituted arenedithiolates [17,18] and napthlalene [18]. Biphenyl, open-bridge complexes have also been reported including biphenyl-2,2-dithiolate [19], tetrachlorobiphenyl-dithiolate [20], $(\mu\text{-S-2-RCONHC}_6H_5)_2$ where R = CH_3, C_6H_5 and 4-FC_6H_4 [21] and others [22]. Wu has reported the synthesis and electrocatalysis of complexes of the form $Fe_2(CO)_6\{\mu\text{-SCH}_2\text{N(R)CH}_2\text{S}\}$ with R = $C_6F_4CF_3$-*p* or $C_6H_4CF_3$-*p* where both electron-withdrawing moieties and a N site for protonation are incorporated into the bridge to achieve a mild reduction potential [23]. Table 1 lists those complexes with the least negative reduction potentials reported to date and which have been tested for catalytic activity using HBF_4 or a similarly strong acid. Chart 2 shows the structures of those compounds included in Table 1.

Here we report the synthesis, electrochemistry and electrocatalytic activity of $Fe_2(CO)_6(\mu\text{-SC}_6F_5)_2$ (**1**) [24–26] where the highly fluorinated bridge is electron-withdrawing, resulting in decreased electron-density at the iron–iron bond. Additionally we discuss the related substituted complexes $Fe_2(CO)_5(PPh_3)(\mu\text{-SC}_6F_5)_2$ (**2**) and $Fe_2(CO)_4(\mu\text{-Ph}_2\text{PCH}_2\text{PPh}_2)(\mu\text{-SC}_6F_5)_2$ (**3**). The structures of these complexes are shown in Section 2.1 below. We address the following points in this paper: (a) whether the electron-withdrawing (SC_6F_5) bridge can lower the overpotential to proton reduction comparable to previously reported complexes; (b) if substitution with phosphine ligands can induce sufficient basicity for protonation across the iron–iron bond; (c) the relative stability of complexes **1**, **2** and **3** to electrochemical reduction and the generation of reduction products that show a high catalytic activity.

2. Results

2.1. Synthesis and characterisation

The hexacarbonyl complex $Fe_2(CO)_6(\mu\text{-SC}_6F_5)_2$ (**1**) is easily prepared as an air-stable bright red solid in good yields upon heating $Fe_3(CO)_{12}$ and pentafluorothiophenol in toluene [24]. The IR spectrum of **1** in dichloromethane shows absorption bands at 2089, 2059, 2022 and 2012 cm^{-1}, representing the stretching modes of the carbonyl ligands. The analogous pdt-bridged complex $Fe_2(CO)_6(\mu\text{-pdt})$ displays absorptions at 2074, 2036 and 1995 cm^{-1} [4a] indicating that the force constant for the CO bonds is increased by substitution of the pdt bridge for the electron-withdrawing SC_6F_5 groups. For such thiolate-bridged complexes *anti* and *syn* isomers are present in solution in equilibrium (Chart 3) as confirmed by the ^{19}F NMR spectrum [27].

A common strategy in the development of hydrogenase biomimics is to sequentially replace one or more carbonyls for the more electron-donating phosphine ligands [9] in order to increase the basicity of the diiron centre and make proton binding more favourable. Heating **1** and a slight excess of PPh_3 in toluene at 80 °C resulted in the slow formation of $Fe_2(CO)_5(PPh_3)(\mu\text{-SC}_6F_5)_2$ (**2**) as a red solid in 26% yield. Complex **2** shows IR absorption bands at lower wavenumbers than **1**: 2058, 2008, 1996, 1981 and 1944 cm^{-1}, carbonyl substitution for PPh_3 as expected increasing the electron-density on diiron centre. In the ^{31}P NMR spectrum two singlets were observed at 29.2 and 65.8 ppm in an approximate 19:1 ratio which we associate with *anti* and *syn* isomers of **2** respectively.

Heating **1** and a slight excess of dppm in toluene for 2 h lead to the formation of an intense red solution from which $Fe_2(CO)_4(\mu\text{-SC}_6F_5)_2(\mu\text{-dppm})$ (**3**) was isolated as a brick red solid in 43% yield. Crystals suitable for X-ray diffraction were grown upon slow diffusion of methanol into saturated dichloromethane solutions and the results of the crystallographic study are summarised in Fig. 1 and its caption (see Supplementary materials for more details). The

Table 1
Table showing the reduction potentials and potential of proton reduction for selected diiron hexacarbonyl complexes. All potentials vs. Fc/Fc^+.

Reference	Bridge	Solvent	$E^{red}_{1/2}$	Acid	*E*cat
[13]	o-Carborane	MeCN	−0.88 V	–	–
[20]	Tetrachlorobiphenyl	DCM	−1.05 V	HBF_4	−1.3 V
	S2C2(CO2Me)2	DCM	−1.11 V	HBF_4	−1.75 V[a]
[15]	3,6-Dichlorobiphenyl	MeCN	−1.20 V	HOTS	−1.20 V
[14]	bdt	MeCN	−1.27 V[b]	HBF_4	−1.27 V
[23]	(μ-SCH2)2N(C6F4CF3-p)	MeCN	−1.54 V	HBF_4	−1.29 V[c]
This work	(SC6F5)2	MeCN	−1.10 V	HBF_4	−1.10 V
		DCM	−1.31 V	HBF_4	−1.31 V

[a] Acid-dependent peak at −1.1 V is not catalytic (ECE).
[b] Ref. [16] reports $E^{red}_{1/2}$ as −1.32 V for this complex.
[c] Protonates at the N, best compared to adt bridged complexes [11].

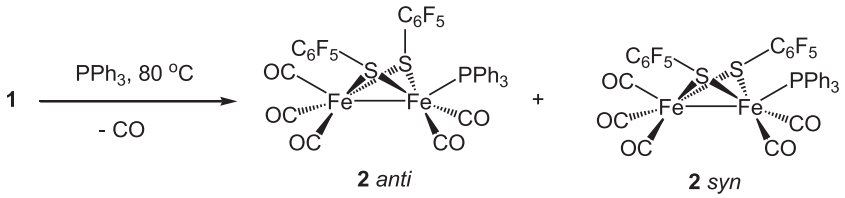

solid-state structure is maintained in solution with both phosphorus atoms being equivalent as shown by the appearance of a singlet at 57.9 ppm in the ^{31}P NMR spectrum. In the IR spectrum carbonyl absorption bands are seen at 2007 m, 1981vs, 1948s, 1926w cm^{-1}.

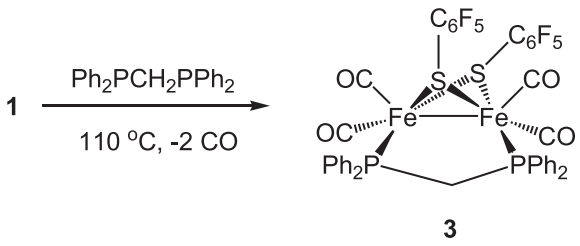

2.2. Protonation studies

Protonation of the diiron centre is a central step in the action of hydrogenase biomimics [8,9] and can readily be followed with IR spectroscopy. Upon protonation, bands corresponding to CO stretching tend to shift to higher wavenumbers as electron-density is withdrawn from the iron–iron bond. Addition of up to 10 equivalents of the strong acid HBF_4-Et_2O to a solution of **1** resulted in no change to the band position or intensity over a 24 h period. This shows that **1** is not protonated under these conditions and also that it is stable in the presence of excess acid. Similarly, upon addition of HBF_4 to **2** or **3** the positions of the bands did not change but over 1 h the intensity of the bands decreased dramatically indicating decomposition of the organometallic complexes in the presence of acid.

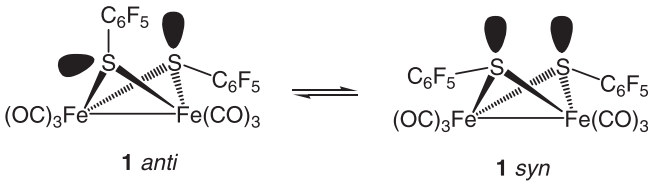

Chart 3.

2.3. Cyclic voltammetry

The cyclic voltammetry (CV) of **1** was carried out in 0.1 M $TBAPF_6$ in dichloromethane both under an argon atmosphere and under CO, as shown in Fig. 2a. Under both conditions, **1** undergoes reduction at $E_{1/2} = -1.31$ V. A further small reduction feature is observed at −1.71 V under argon only, followed by an additional larger reduction peak at −2.15 V, which is present under both argon and CO. Several small anodic peaks occur at −0.65 V, −0.50 V and 0.65 V, probably related to decomposition products of the irreversible reduction processes. When scanning first towards positive potentials the neutral complex begins to undergo oxidation at ca. 1 V close to the edge of the available potential window in dichloromethane (not shown). The CV of **1** was also carried out in the coordinating solvent MeCN in order to better compare the reduction potential obtained with those of other researchers [13–15,20,23]. Broadly similar behaviour was observed as in dichloromethane, but with the irreversible reduction occurring at −1.10 V, rather than −1.31 V (see Supplementary materials). Comparison with the reduction potentials of other reported complexes in Table 1 shows that **1** undergoes reduction at potentials comparable to

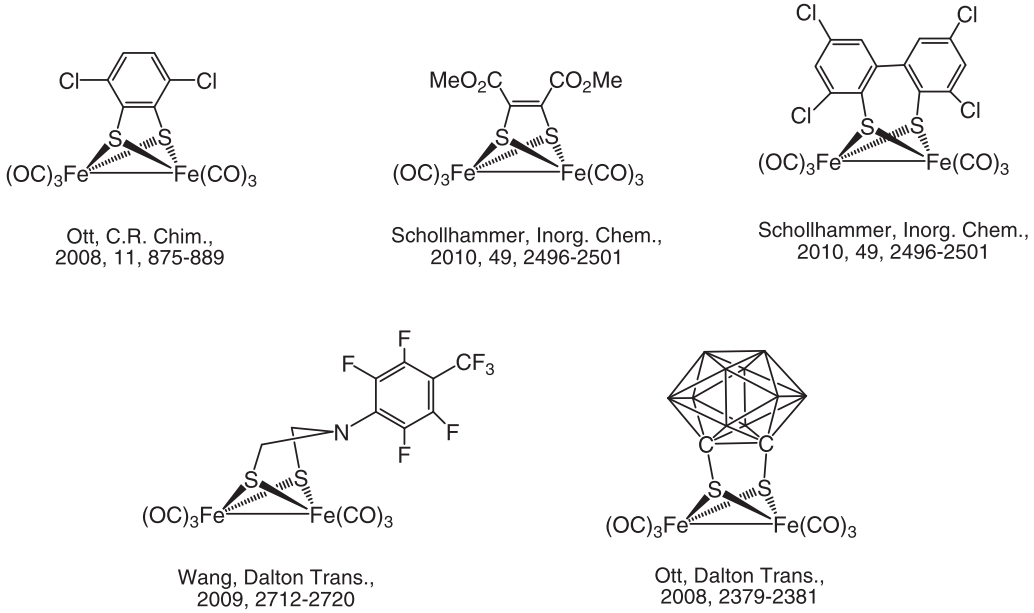

Chart 2.

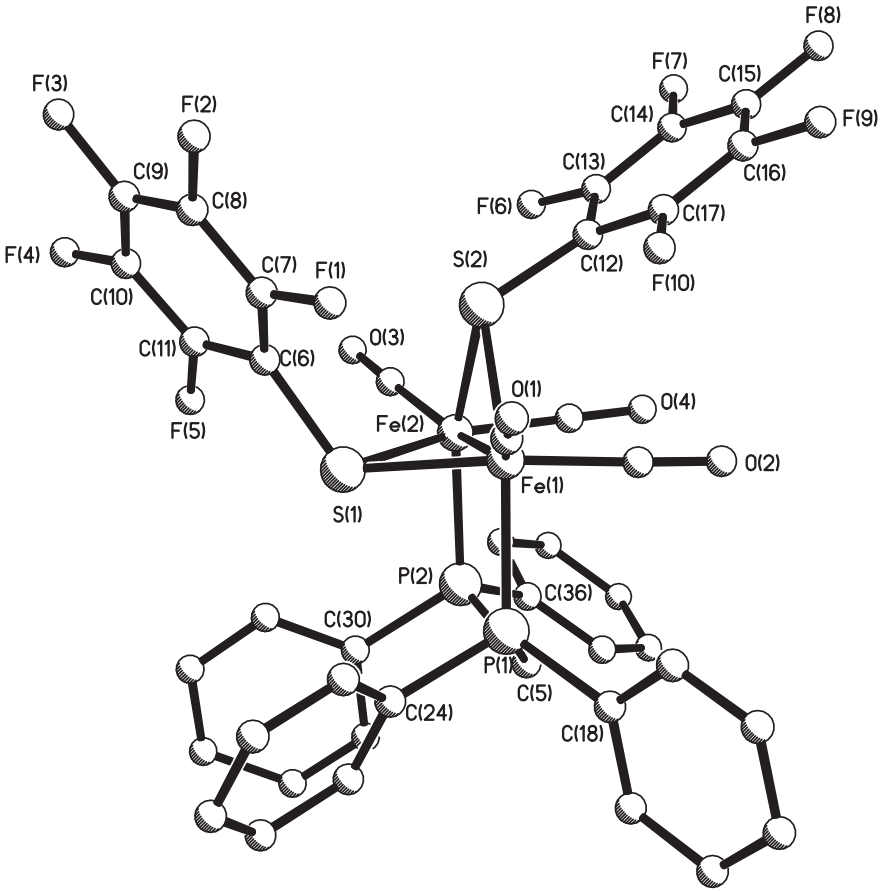

Fig. 1. Molecular structure of $Fe_2(CO)_4(\mu\text{-dppm})(\mu\text{-}SC_6F_5)_2$ (**3**). Hydrogen atoms are omitted for clarity. Selected bond distances (Å) and angles (°): Fe(1)–Fe(2) 2.501(1), Fe(1)–S(1) 2.282(2), Fe(2)–S(1) 2.300 (2), Fe(1)–S(2) 2.272(2), Fe(2)–S(2) 2.276 (1), Fe(1)–P(1) 2.228(1), Fe(2)–P(2) 2.228(2), P(1)–Fe(1)–Fe(2) 96.57(5), P(1)–Fe(1)–S(1) 86.40(5), P(1)–Fe(1)–S(2) 153.29(6), P(1)–Fe(1)–C(1) 100.6 (2), P(1)–Fe(1)–C(2) 88.5(2), Fe(1)–S(1)–Fe(2) 66.15(4), Fe(1)–S(2)–Fe(2) 66.72(4), S(1)–Fe(1)–Fe(2) 57.27(4), S(1)–Fe(2)–Fe(1) 56.58(4), S(1)–Fe(1)–S(2) 78.41(5), P(1)–C(5)–P(2) 112.9(3), Fe(1)–S(1)–C(6) 116.6 (2), Fe(1)–S(2)–C(12) 116.8 (2).

the tetrachlorobiphenyl-thiolate and $S_2C_2(CO_2Me)_2$ bridged complexes reported by Schollhammer [20].

The reduction behaviour of **1** was investigated over a range of scan rates from 0.01 to 10 V s^{-1}. Fig. 2c shows the reduction response normalised by division by the square root of scan rate for scan rates of 0.05 and 1.0 V s^{-1}. The normalised currents at the slower scan rate tend to twice those at faster scan rates, indicating a transition from a one to a two electron reduction. This behaviour has been reported previously for $Fe_2(CO)_6(\mu\text{-edt})$ reduction and attributed to a potential inversion mechanism [28], where structural changes after addition of the first electron enables uptake of the second electron at potentials less negative than the first. Therefore on a voltammetric timescale comparable to the rate of structural change an overall two electron reduction can take place, but at fast scan rates the structural change does not have time to take place and reduction is limited to the addition of the first electron only. A similar mechanism may be taking place here; addition of an electron leads to an unstable anion species, which undergoes further reaction. Interestingly some reversibility is observed at slower scan rates, indicating that although two electron uptake is associated with structural change, on a slow voltammetric timescale this may be reversible. To explore possible mechanisms for this structural change the experiment was repeated in CO saturated solution. Loss of a carbonyl is a common result of reduction of similar diiron hexacarbonyl species [8] but this can be suppressed by performing experiments in a CO saturated solution if the CO loss is reversible. However, as is clear from Fig. 2a, in this case no improvement in reversibility was observed in CO, indicating that ligand loss is unlikely to be the sole structural change. Under CO the only difference observed was the absence of the small reduction peak at −1.71 V, which is attributed to a reduction product and is discussed further below.

Investigation of mono-substituted **2** by CV (see Supplementary materials) showed that the complex undergoes irreversible reduction at −1.53 V in dichloromethane, with a further small reduction peak noted at −1.94 V. Irreversible oxidation of **2** is observed at 0.86 V when scanning first towards positive potentials. The shift of the reduction peak negative by 0.16 V compared to **1** and the appearance of the oxidation peak within the solvent potential window are due to the increased electron-density on the diiron centre from the PPh_3 ligand. The disubstituted complex **3** is expected to exhibit even more negative reduction potentials than **2** and this is observed (Fig. 2b). The reduction of **3** shows similar scan rate dependence to **1**, with a transition from one to two electron reduction as scan rate is decreased (see Fig. 2d). However for **3** the one electron reduction at faster scan rates exhibits some reversibility which was not the case for **1**. It seems that the bridging diphosphine is able to confer some structural stability to $\mathbf{3}^-$ and is able to inhibit some structural change from taking place after addition of one electron.

2.4. Electrocatalysis

Under an argon environment the currents at the potential of the first reduction of complex **1** increase on sequential addition of equivalents of HBF_4 as shown in Fig. 3a. The increase in cur-

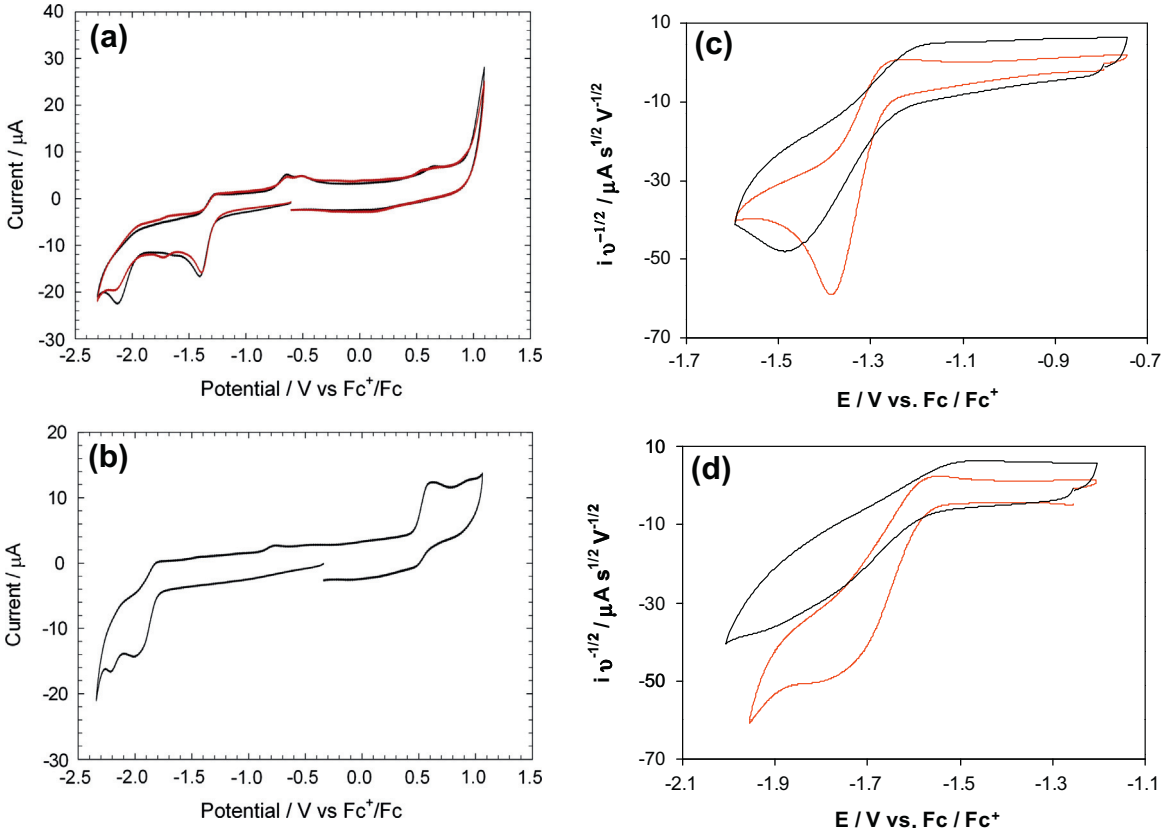

Fig. 2. (a) CV at 0.1 V s^{-1} of 0.5 mM complex **1** in 0.1 M $TBAPF_6$ in dichloromethane under argon (brown) and under CO (black); (b) CV at 0.1 V s^{-1} of 0.5 mM complex **3** in 0.1 M $TBAPF_6$ in dichloromethane under argon; (c) CV at 0.05 V s^{-1} (red) and 1.0 V s^{-1} (black) of **1** over potential range of first reduction peak, with current normalised by division by $v^{1/2}$; (d) CV at 0.05 V s^{-1} (red) and 1.0 V s^{-1} (black) of **3** over potential range of first reduction peak, with current normalised by division by $v^{1/2}$. (For interpretation of the references to colour in this figure legend, the reader is referred to the web version of this article.)

rent at the potential of the first reduction peak is consistent with an EC mechanism, where $\mathbf{1}^-$ is generated at the electrode, is basic enough to protonate and then supports a catalytic mechanism. Interestingly a substantial increase in current is also noted at ~−1.7 V. This is the potential at which the small reduction peak is noted in the absence of CO (Fig. 2a). The species that undergoes reduction at this potential is clearly highly catalytic based on the catalytic currents achieved for the small quantity of material in solution. Further catalytic processes, attributed to a further reduction and protonation of the complex are noted below −2 V and are overlaid on increased background currents due to the direct reduction of the acid at the electrode that takes place at these potentials.

The catalytic studies were continued with the sequential addition of the weaker acetic acid to **1** in an argon saturated solution, shown in Fig. 3b for the addition of 10 equivalents of acetic acid. As reported for similar electron-poor complexes [15,16,19], catalysis takes place minimally at the potential of the first reduction under these conditions. It is clear that $\mathbf{1}^-$ is not sufficiently basic to protonate in the presence of the weaker acid. In contrast, increased currents are observed at −1.7 V on addition of acid, indicating that the catalytic reduction product noted above is more basic than $\mathbf{1}^-$ and is still an efficient catalyst under these milder conditions. Catalysis is also observed at −2.1 V which seems to be associated with further reduction products of $\mathbf{1}^-$. The role of the −1.7 V species in catalysis was explored further by repeating the addition of acetic acid in a CO-saturated dichloromethane solution. Catalysis at −1.7 V is *not* observed under these conditions (see Supplementary materials), but increased currents are still seen at −2.1 V. This confirms that the catalytic species at −1.7 V is only formed in the absence of CO as discussed above.

Complexes **2** and **3** were also tested for catalytic activity towards proton reduction in the presence of HBF_4. The rationale behind substitution of CO for phosphine ligands is that addition of electron-density to the iron–iron bond may promote protonation. If protonation of the neutral complex occurs the potential for onset of proton reduction catalysis is usually shifted to less negative potentials, which is the desired outcome. However IR studies have shown that **2** and **3** do not readily protonate and electrochemical studies support this conclusion. Complex **2** appears particularly unstable, as after addition of just one equivalent of HBF_4 the reduction peak for the neutral complex is no longer present. Instead, enhanced currents are noted at the potential of the small, second reduction peak at −1.94 V (see Supplementary materials). We therefore speculate that, as observed for **1** above, a decomposition product is formed (in this case induced by addition of acid) that is readily protonated and undergoes a catalytic cycle. This species might be expected to have similarities to the catalytic product of **1** discussed above. Complex **3** was more stable in acid and catalysis was observed at −1.9 V, the position of the reduction of the neutral complex (see Supplementary materials). Thus although **3** is more electron-rich than **1** it is not sufficiently basic to allow protonation before electrochemical reduction. This is consistent with previous studies of phosphine-substituted complexes with electron-withdrawing bridges [16,22,23]. Within the available potential window, additional catalytic processes at more negative potentials are not apparent. This would suggest that a catalytic decomposition product is not formed after reduction of **3** and this may be due to the stability inferred by the bridging diphosphine ligand inhibiting bond cleavage and fragmentation. This is also consistent with the reduction behaviour of **3**, where the one electron reduction was noted to be more reversible than the one electron reduction of **1**.

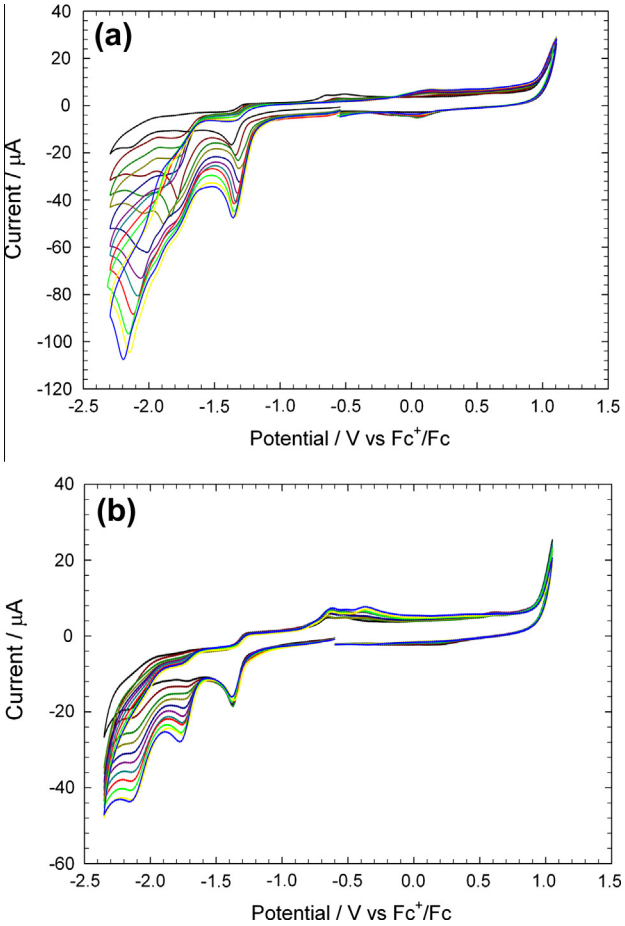

Fig. 3. (a) CVs at 100 mV s^{-1} of 0.5 mM complex **1** with sequential addition of 1–10 equivalents of HBF_4 in dichloromethane under argon; (b) CVs at 100 mV s^{-1} of 0.5 mM complex **1** with sequential addition of 1–10 equivalents of acetic acid in dichloromethane under argon.

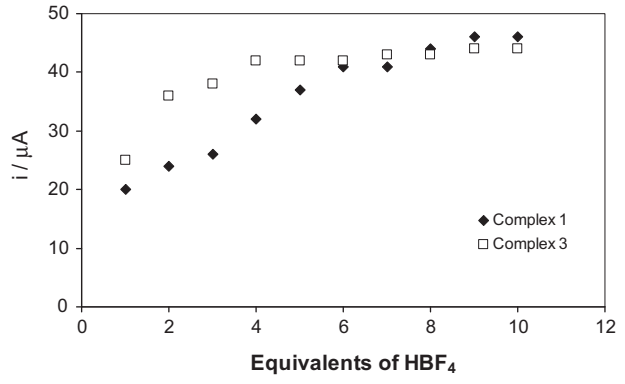

Fig. 4. Plot of electrocatalytic peak current at potential of first reduction vs. equivalents of HBF_4 added for complex **1** (filled diamonds) and complex **3** (open squares).

The catalytic limiting current values for 1 and 3 with up to 10 equivalents of HBF_4 are plotted in Fig. 4, where it is clear that for 3 limiting current becomes independent of acid concentration after addition of only four acid equivalents. This suggests that the rate-limiting step in the catalytic cycle is acid-independent and is likely to be elimination of the hydrogen molecule and regeneration of the neutral catalytic species, as noted in earlier studies of phosphine-substituted complexes [12]. In contrast, limiting currents do not reach a maximum limit for 1 after addition of 10 equivalents of acid. The catalytic current for an E initiated catalytic cycle can be quantified using Eq. (1), where n is the stoichiometric number of electrons involved in catalysis, *F* is Faraday's constant, *A* is the area of the electrode, *D* is the diffusion coefficient of the catalyst, *k* is the rate constant of the catalytic process and *y* is the order of the reaction with respect to the substrate (the acid in this case):

$$i_{cat} = n\ F\ A[\mathrm{Cat}]D^{1/2}k^{1/2}[HBF_4]^{y/2} \quad (1)$$

When the catalytic current becomes independent of acid concentration as noted for 3, the order y with respect to the acid concentration becomes zero, and this equation can be re-written as Eq. (1a):

$$i_{cat} = n\ F\ A[\mathbf{3}]D^{1/2}k^{1/2} \quad (1a)$$

Given an overall two electron process and approximating D to 1×105 cm s−1, a rate constant for the elimination of H2 rate-limiting step can be determined as k ~ 3.5 s−1. This value is within the same order of magnitude as reported for diphosphine-substituted pdt complexes [12]. As catalytic current remains dependent of [HBF4] for complex 1 it can be assumed that H2 elimination is not rate-limiting for this complex under these conditions and the rate constant for the H2 elimination step will be considerably higher.

2.5. Simulations of catalytic processes

To gain further insight into the relative rates of the catalytic processes, and especially to probe the reactivity of the catalytic reduction product (represented as species **A** in further discussion) relative to **1**, DigiSim simulations were carried out using the catalytic cycles outlined in Fig. 5a. Simulated CVs for **1** with no acid, 2 and 10 equivalents of HBF_4 are shown in Fig. 5b and those for **1** with no acid, 2 and 10 equivalents of acetic acid are shown in Fig. 5c. Catalytic processes below −2 V have not been included in the simulation and neither have the currents attributed to direct reduction of the acid at the electrode. The exact parameters used in the simulations are given in Supplementary materials, however the parameters providing the most insight into the mechanisms are the relative equilibrium constants, *K* and rate constants, *k*, for the two protonation steps and *k* for the H_2 elimination step.

An ECEC mechanism is simulated for both **1** and **A** and the simulated CVs that provide the best reflection of the experimental results in terms of limiting currents, acid concentration dependence and relative contributions from the two catalytic processes are when $k_1 = k_2 = 1 \times 10^6$ mol^{-1} dm^3 s^{-1}; $K_1 = K_2 = 1 \times 10^{10}$ mol^{-1} dm^3; $k_4 = k_5 = 1 \times 10^8$ mol^{-1} dm^3 s^{-1} and $K_4 = K_5 = 1 \times 10^{15}$ mol^{-1} dm^3 using HBF_4 as the proton source. The rate constants are the lower limit values; in other words if the k values are increased there is no influence on the simulated voltammogram obtained. It becomes clear from these values that **A** shows much enhanced catalytic currents (relative to its concentration in solution) primarily because the equilibrium constant for protonation of $\mathbf{A}^-$ (K_4) is 1×10^5 larger than that for protonation of $\mathbf{1}^-$ (K_1) and that its rate constant for protonation (k_4) is 100 times faster than for $\mathbf{1}^-$ (k_1). This shows that the protonation equilibrium is more in favour of the protonated species, i.e. that $\mathbf{A}^-$ is more basic than $\mathbf{1}^-$, and also that it protonates more rapidly. This could be because $\mathbf{A}^-$ has a vacant coordination site, or that protonation is less sterically hindered. The rate constants obtained for the H_2 elimination step are 1800 s^{-1} for **1** (k_3) and 100 s^{-1} for **A** (k_6), which may suggest that species **A** can bind the hydrogen molecule more strongly than **1**.

The CV response of **3** was also simulated with HBF_4 as the proton source, with the increased electron-density at the iron–iron bond reflected in larger equilibrium and rate constants for

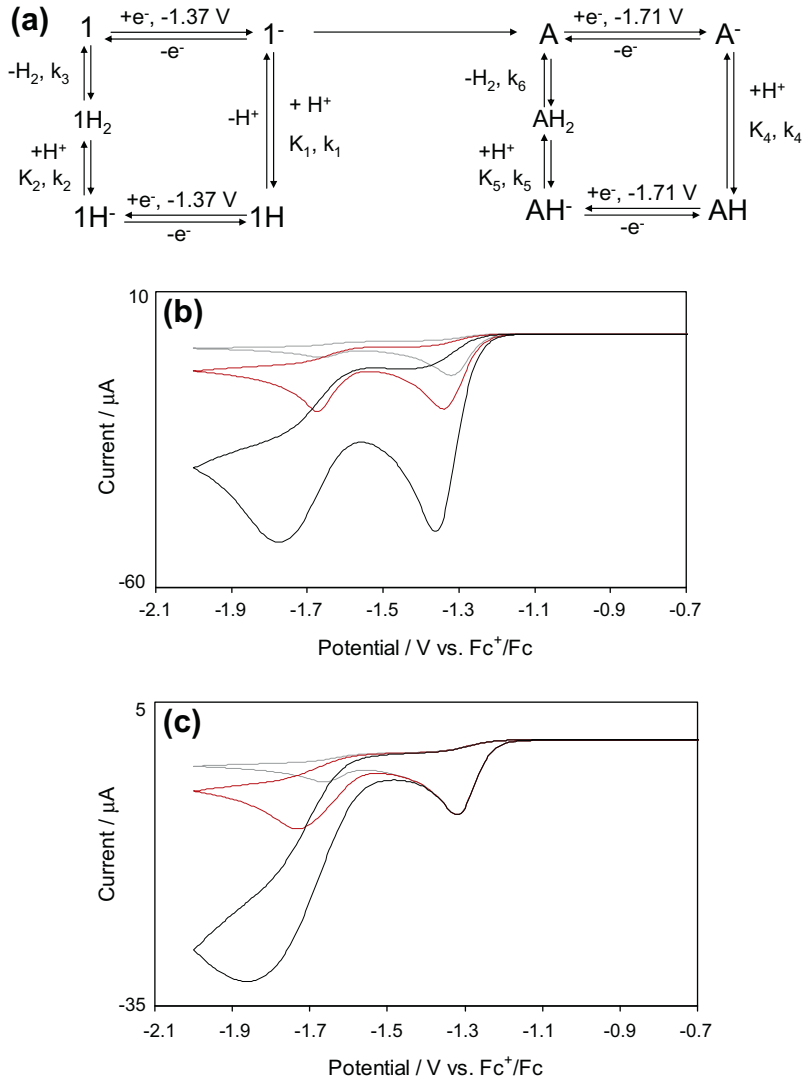

Fig. 5. (a) Reaction mechanism used to simulate electrocatalytic response of complexes **1** in the presence of acid. **1** represents the neutral catalyst complex, **A** indicates the catalytic species undergoing reduction at −1.71 V, *K* and *k* represent equilibrium constants and forward rate constants for the respective reaction steps; (b) Simulated CVs for 0.5 mM **1** with addition of 2 and 10 equivalents of strong acid (HBF_4) and (c) Simulated CVs for 0.5 mM **1** with addition of 2 and 10 equivalents of weak acid (acetic acid).

protonation than **1**: $K_1 = K_2 = 1 \times 10^{11}$ mol^{-1} dm^3 and $k_1 = k_2 = 6 \times 10^6$ mol^{-1} dm^3 s^{-1}. The best fit to experimental limiting currents was obtained when the rate constant for H_2 elimination from **3** (k_3) was found to be 10 s^{-1}, which is considerably lower than the 1800 s^{-1} value obtained for **1**; this is in reasonable agreement with the value of 3.5 s^{-1} obtained from the experimental limiting currents in Fig. 4 above. This value is consistent with stronger bonding of the hydrogen molecule to complex **3**.

The CVs for **1** with acetic acid as the proton source were also simulated, where the best match to experiment was obtained for $k_1 = k_2 = 1 \times 10^6$ mol^{-1} dm^3 s^{-1}; $K_1 = K_2 = 10$ mol^{-1} dm^3; $K_4 = K_5 = 1 \times 10^5$ mol^{-1} dm^3 and $k_4 = k_5 = 1 \times 10^8$ mol^{-1} dm^3 s^{-1}. This is consistent with the conclusions above; it is the relative equilibrium and rate constants for protonation of $\mathbf{1}^-$ and $\mathbf{A}^-$ that influences the relative catalytic currents for the two species. In this case $\mathbf{1}^-$ is not basic enough to be protonated by acetic acid while $\mathbf{A}^-$ is; hence catalysis only takes place at −1.7 V.

3. Discussion

The initial motivation of this study was to produce a diiron hydrogenase model complex with a more positive reduction potential than obtained to date. Although **1** undergoes reduction at quite mild potentials (−1.31 V in dichloromethane, −1.10 V in acetonitrile) there are other reported complexes that undergo reduction at this potential or even slightly more positive of this (see Table 1) [20]. As complex **1** is not sufficiently basic it will not protonate in its neutral form, but must first undergo electrochemical reduction to its anion. Attempts to increase the basicity of the complex by mono- and disubstitution with phosphines did not result in protonation of complexes **2** and **3** but instead resulted in more negative reduction potentials for the complexes.

Although this study was not wholly successful in its first objective it has revealed some interesting pointers towards design of new catalysts. Complexes **1** and **2** both generate on reduction sub-stoichiometric quantities of a highly catalytic species that is more basic than the parent species and also protonates more rapidly. The production of this species is suppressed in the presence of CO. One possible reaction pathway is fragmentation of the parent molecule, via cleavage of the iron–iron bond, to produce a mononuclear complex. The inhibition of its reduction chemistry in CO saturated solution suggests that a vacant coordination site is required for it to perform as a catalyst and this is ligated and blocked in the presence of excess CO. The electron-withdrawing nature of the SC_6F_6 moieties removes electron-density from the metal–metal

bond and encourages fragmentation of the molecule. The open structure of the bridge also allows fragmentation to mononuclear species which may be prevented in the pdt and adt analogues. In support of this mechanism complex **3** does not show evidence of generation of the putative catalytic species on reduction, which indicates that the bridging diphosphine ligand imparts stability and prevents fragmentation.

Our attempts to synthesise a chelating diphosphine analogue of **3**, which would provide asymmetric electron-density along the iron–iron bond and a possible route to protonation in the neutral form, were unsuccessful. Instead we observed the preferential formation of a mononuclear species similar in structure to the putative catalytic species **A** discussed above. We are currently investigating its identity and electrocatalytic properties, the results of which will be reported elsewhere. In the past few years examples of mononuclear iron (II) complexes [29] with vacant coordination sites [30] have been reported that can catalyse proton reduction at mild overpotentials. These complexes mimic the distal Fe of the diiron H cluster, where hydride binding and electron transfer are believed to exclusively take place in the hydrogenase enzyme. Thus it may be the case that faithful structural models of the diiron cluster are unnecessary for efficient homogeneous catalysis of proton reduction and fragments of the active site may perform as well if not better. The serendipitous generation of putative mononuclear reactive products from our fluorinated diiron complexes has suggested a new series of complexes to investigate.

An alternate explanation for the catalytic process at −1.7 V is reduction of the $\mathbf{1H}^-$ species, followed by its subsequent protonation and hydrogen elimination. $\mathbf{1H}^-$ is generated by the protonation of the $\mathbf{1}^{2-}$ species, which as we have seen from the scan rate studies is perhaps the dominant reduction product at slower voltammetric timescales. We carry out the catalysis studies at 0.1 V s^{-1}, where reduction currents are intermediate between those of a one or two electron transfer. The most likely product of the two electron reduction product of $Fe(CO)_6(\mu\text{-bdt})$ [16] has been calculated to have a vacant coordination site due to the cleavage of the Fe–S bond of the bridge and a similar structure for $\mathbf{1}^{2-}$ would be expected to be highly basic and to protonate quickly in weak acid. Additionally the presence of excess CO in solution may result in this site being ligated and thus suppress the catalytic response. It is difficult at this stage to unequivocally determine the identity of the catalytic species; regardless both possibilities highlight the importance of a vacant coordination site.

4. Conclusions

Here we report the synthesis, characterisation, electrochemistry and electrocatalysis of diiron complexes with a highly fluorinated, electron-withdrawing dithiolate bridge. The complex was able to catalyse proton reduction at the potential at which it underwent reduction, representing a relatively small overpotential. Introducing phosphine ligands into the structure unfortunately did not improve the catalytic performance as the complexes were still not basic enough to protonate in their neutral form. However, an interesting prospect for further investigation was the highly catalytic product formed after reduction of the diiron complexes. A comparison using simulation of the rate constants and equilibrium constants for protonation of the initial diiron complex and this product revealed that was considerably more basic and its protonation very facile. Possible identities for this highly catalytic species are (i) a mononuclear iron species formed after Fe–Fe bond cleavage of the parent molecule or (ii) the $\mathbf{1}^{2-}$ species with a vacant coordination site generated by the breaking of an Fe–S bond.

5. Experimental

5.1. Methods and materials

All reactions were carried out using standard Schlenk-line techniques under N_2 and reaction solvents were purified on alumina columns. Work-up was done in air using standard bench reagents. NMR spectra were run on a Bruker AMX400 spectrometer and referenced internally to the residual solvent peak (^1H) or externally to $P(OMe)_3$ (^{31}P). Infrared spectra were run on a Nicolet 205 FT-IR spectrometer in a solution cell fitted with calcium fluoride plates, subtraction of the solvent absorptions being achieved by computation. Fast atom bombardment mass spectra were recorded on a VG ZAB-SE high resolution mass spectrometer and elemental analyses were performed in house. Triphenylphosphine (PPh_3) and bis(diphenylphosphino)methane (dppm) were purchased from Aldrich and used without further purification. $Fe_3(CO)_{12}$ was purchased from Alfa Aesar (Johnson Matthey) and used as received. $Fe_2(CO)_6(\mu\text{-}SC_6F_5)_2$ (**1**) was prepared by a slight modification of the method reported by Stone [24].

5.2. Synthesis of $Fe_2(CO)_6(\mu\text{-}SC_6F_5)_2$ (**1**)

$Fe_3(CO)_{12}$ (1.50 g, 2.98 mmol) and C_6F_5SH (1.79 ml, 5.96 mmol) were refluxed in toluene (50 cm^3) for 1 h, the dark green solution turning deep red. The solution was cooled to room temperature and removal of volatiles yielded a red oily solid. This was dissolved in hexanes and filtered, removal of volatiles from the clear red filtrate gave a bright red solid (0.84 g, 0.57 mmol, 29%). The solid caught in the filter paper was dissolved in CH_2Cl_2, and on removal of volatiles yielded a bright red solid (1.61 g, 52%). IR analysis confirmed the two solids to be the same compound, giving the overall yield (2.44 g, 3.61 mmol, 81%). IR ν(CO)(CH_2Cl_2) 2089m, 2059vs, 2022s, 2012s cm^{-1}; IR ν(CO)(hexane) 2090m, 2062vs, 20272s, 2014s, 2010sh cm^{-1}.

5.3. Synthesis of $Fe_2(CO)_5(\mu\text{-}SC_6F_5)_2(PPh_3)$ (**2**)

A toluene (20 cm^3) solution of $Fe_2(CO)_6(\mu\text{-}SC_6F_5)_2$ (**1**) (100 mg, 0.15 mmol) and PPh_3 (50 mg, 0.19 mmol) was heated for 7 h maintaining bath temperature at 80 °C. The reaction mixture was allowed to cool at room temperature and filtered through a filter paper. The solvent was removed from the filtrate by rotary evaporation under vacuum and the residue again dissolved in hexane which was kept in refrigerator for crystallization at 4 °C. $Fe_2(CO)_5(PPh_3)(\mu\text{-}SC_6F_5)_2$ (**2**) (35 mg, 26%) was obtained as deep red needles after several days. IR ν(CO)(CH_2Cl_2): 2059s, 2009vs, 1997s, 1981m, 1945w cm^{-1}. IR ν(CO)(hexane): 2068s, 2061s, 2017s, 2012s, 2000s, 1985sh, 1983ms, 1956w, 1950w cm^{-1}. ^1H NMR ($CDCl_3$): δ 7.69–7.49 (m, 15 H). $^{31}P\{^1H\}$ NMR ($CDCl_3$): δ 29.2 (s) (major, 95%); 65.8 (s) (minor, 5%). Anal. Calcd. for $C_{35}H_{15}F_{10}Fe_2O_5P_1S_2.0.5C_6H_{14}$: C, 47.74; H, 2.61. Found: C, 48.03; H, 1.99%.

5.4. Synthesis of $Fe_2(CO)_4(\mu\text{-}SC_6F_5)_2(\mu\text{-dppm})$ (**3**)

$Fe_2(CO)_6(\mu\text{-}SC_6F_5)_2$ (0.33 g, 0.48 mmol) and dppm (0.21 g, 0.55 mmol) were refluxed in toluene (30 cm^3) for 2 h, the dark red solution turning a deeper red. The solution was cooled to room temperature and volatiles were removed yielding a dark red oily solid. This was washed with hexanes and recrystallised from CH_2Cl_2–MeOH giving deep red block crystals (0.53 g. 43%). IR ν(CO)(CH_2Cl_2) 2007 m, 1981vs, 1948s, 1926w; ^1H NMR ($CDCl_3$) δ 7.66–7.05 (m, 20H, Ph), 4.37 (q, *J* 12.0, 1H, CH_2), 3.60 (q, *J* 12.0, 1H, CH_2); ^{31}P NMR ($CDCl_3$) δ 57.9 (s); Mass spectrum (FAB^+): 1007 ($M + H^+$), 950 (M − 2CO), 894 (M − 4CO); Elemental analysis

found: C 46.90, H 2.14; Calc. for $Fe_2S_2P_2O_4F_{10}C_{41}H_{22}\cdot CH_2Cl_2$: C 46.20, H 2.20.

5.5. Electrochemical studies

Electrochemistry was carried out predominantly in deoxygenated dichloromethane solutions with 0.1 M $TBAPF_6$ as supporting electrolyte. Some experiments were also carried out in acetonitrile to compare reduction potential values with those reported in literature. The working electrode was a 3 mm diameter glassy carbon electrode which was polished with 0.3 μm alumina slurry prior to each scan. The counter electrode was a Pt wire and the quasi-reference electrode was a silver wire. All CVs were referenced to the Fc/Fc^+ redox couple. An Autolab potentiostat (EcoChemie, Netherlands) was used for all electrochemical measurements. Catalysis studies were carried out by adding equivalents of HBF_4-Et_2O (Sigma–Aldrich). Simulation of the catalytic responses of complexes **1** and **3** in the presence of HBF_4 was carried out using DigiSim version 3.0.

5.6. X-ray data collection and solution

Single crystal of **3**·CH_2Cl_2 was mounted on glass fibre and all geometric and intensity data were taken from this sample using a Bruker SMART APEX CCD diffractometer using graphite-monochromated Mo Kα radiation ($\lambda = 0.71073$ Å) at 150 ± 2 K. Data reduction was carried out with SAINT PLUS and absorption correction applied using the programme SADABS. Structures were solved by direct methods and developed using alternating cycles of least-squares refinement and difference-Fourier synthesis. All non-hydrogen atoms were refined anisotropically. Hydrogens were placed in calculated positions (riding model). Structure solution used SHELXTL PLUS V6.10 program package. The crystal was only weakly diffracting and hence we were unable to collect useful high angle data. Consequently the only 90.9% of the total reflections were measured. Nevertheless, the data measured was of reasonable quality (Rint = 0.0294) and the solution presented is reliable.

Crystallographic data for $Fe_2(CO)_4(\mu\text{-dppm})(\mu\text{-}SC_6F_5)_2$ (**3**)·CH_2Cl_2: red block, dimensions 0.46 × 0.28 × 0.24 mm^3, triclinic, space group *P*1*bar*, $a = 10.416(2)$, $b = 11.641(3)$, $c = 18.723(4)$ Å, $\alpha = 87.951(4)$, $\beta = 82.291(4)$, $\gamma = 77.182(4)^\circ$, $V = 2193.6(9)$ $Å^3$, $Z = 2$, $F(000)$ 1092, $d_{calc} = 1.652$ g cm^{-3}, $\mu = 1.036$ mm^{-1}. 13,393 reflections were collected, 8905 unique [R(int) = 0.0294] of which 6888 were observed [$I > 2.0\sigma(I)$]. At convergence, $R_1 = 0.0749$, $wR_2 = 0.2423$ [$I > 2.0\sigma(I)$] and $R_1 = 0.0939$, $wR_2 = 0.2841$ (all data), for 577 parameters. CCDC 929180.

Acknowledgements

We thank University College London for the provision of a studentship (DU), the EPSRC for an Advanced Fellowship (KBH) and a post-doctoral fellowship (NH) and the Commonwealth Scholarships Commission for a studentship (SG).

Appendix A. Supplementary material

Supplementary data associated with this article can be found, in the online version, at http://dx.doi.org/10.1016/j.jelechem.2013.05.018.

References

[1] (a) J.W. Peters, Curr. Opin. Struct. Biol. 9 (1999) 670–676;
(b) A.L. De Lacey, V.M. Fernandez, M. Rousett, R. Cammack, Chem. Rev. 107 (2007) 4304–4330.
[2] K.A. Vincent, A. Parkin, F.A. Armstrong, Chem. Rev. 107 (2007) 4366–4413.
[3] For a review see: J.-F. Capon, F. Gloaguen, P. Schollhammer, J. Talarmin, Coord. Chem. Rev. 249 (2005) 1664–1676.
[4] (a) A. Le Cloirec, S.P. Best, S. Borg, S.C. Davies, D.J. Evans, D.J. Hughes, C.J. Pickett, Chem. Commun. (1999) 2285–2287;
(b) E.J. Lyon, I.P. Georgakaki, J.H. Reibenspies, M.Y. Darensbourg, Angew. Chem. Int. Ed. 38 (1999) 3178–3180;
(c) M. Schmidt, S.M. Contakes, T.B. Rauchfuss, J. Am. Chem. Soc. 121 (1999) 9736–9737.
[5] C. Tard, X.M. Liu, S.K. Ibrahim, M. Buschi, L. De Gioia, S.C. Davies, X. Yang, L.S. Wang, G. Sawer, C.J. Pickett, Nature 433 (2005) 610–613.
[6] S. Dey, A. Rana, S.G. Dey, A. Dey, ACS Catal. 3 (2013) 429–436.
[7] S.L. Matthews, D.M. Heinekey, Inorg. Chem. 49 (49) (2010) 9746–9748.
[8] (a) J.-F. Capon, F. Gloaguen, F.Y. Petillon, P. Schollhammer, J. Talarmin, Coord. Chem. Rev. 253 (2009) 1476–1494;
(b) D. Chong, I.P. Georgakaki, R. Mejia-Rodriguez, J. Sanabria-Chinchilla, M.P. Soriaga, M.Y. Darensbourg, Dalton Trans. 21 (2003) 4158–4163;
(c) J.-F. Capon, F. Gloaguen, P. Schollhammer, J. Talarmin, J. Electroanal. Chem. 566 (2004) 241–247.
[9] For selected examples see: (a) J.-F. Capon, F. Gloaguen, F.Y. Pétillon, P. Schollhammer, J. Talarmin, Eur. J. Inorg. Chem. (2008) 4671–4681;
(b) F.I. Adam, G. Hogarth, I. Richards, J. Organomet. Chem. 692 (2007) 3957–3968;
(c) F.I. Adam, G. Hogarth, S.E. Kabir, I. Richards, C.R. Chim. 11 (2008) 890–905;
(d) W. Gao, J. Ekström, J. Liu, C. Chen, L. Eriksson, L. Weng, B. Åkermark, L. Sun, Inorg. Chem. 46 (2007) 1981–1991;
(e) A. K Justice, G. Zampella, L. De Gioia, T.B. Rauchfuss, J.I. van der Vlugt, S.R. Wilson, Inorg. Chem. 46 (2007) 1655–1664;
(f) N. Wang, M. Wang, T. Liu, T. Zhang, M. Darensbourg, L. Sun, Inorg. Chem. 47 (2008) 6948–6955.
[10] (a) J.A. Wright, C.J. Pickett, Chem. Commun. (2009) 5719–5721;
(b) A. Jablonskyte, J.A. Wright, C.J. Pickett, Dalton Trans. 39 (2010) 3026–3034.
[11] G.A.N. Felton, C.A. Mebi, B.J. Petro, A.K. Vannucci, D.H. Evans, R.S. Glass, D.L. Lichtenberger, J. Organomet. Chem. 694 (2009) 2691–2699.
[12] (a) J.L. Stanley, Z.M. Heiden, T.B. Rauchfuss, S.R. Wilson, L. De Gioia, G. Zampella, Organometallics 27 (2008) 119–125;
(b) G. Eilers, L. Schwartz, M. Stein, G. Zampella, L. De Gioia, S. Ott, R. Lomoth, Chem. Eur. J. 13 (2007) 7075–7084;
(c) J.-F. Capon, S. Ezzaher, F. Gloaguen, F.Y. Petillon, P. Schollhammer, J. Talarmin, Chem. Eur. J. 14 (2008) 1954–1964.
[13] L. Schwartz, L. Eriksson, R. Lomoth, F. Teixidor, C. Vinas, S. Ott, Dalton Trans. (2008) 2379–2381.
[14] J.-F. Capon, F. Gloaguen, P. Schollhammer, J. Talarmin, J. Electroanal. Chem. 595 (2006) 47–52.
[15] L. Schwartz, P.S. Singh, L. Eriksson, R. Lomoth, S. Ott, C.R. Chim. 11 (2008) 875–889.
[16] G.A.N. Felton, A.K. Vannucci, J. Chen, L.T. Lockett, N. Okumura, B.J. Petro, U.I. Zakai, D.H. Evans, R.S. Glass, D.L. Lichtenberger, J. Am. Chem. Soc. 129 (2007) 12521–12530.
[17] E.S. Donovan, J.J. McCormick, G.S. Nichol, G.A.N. Felton, Organometallics 31 (2012) 8067–8070.
[18] C.A. Mebi, D.S. Karr, B.C. Noll, Polyhedron 50 (2013) 164–168.
[19] P.S. Singh, H.C. Rudbeck, P. Huang, S. Ezzaher, L. Eriksson, M. Stein, S. Ott, R. Lomoth, Inorg. Chem. 48 (2009) 10883–10885.
[20] K. Charreteur, M. Kdider, J.-F. Capon, F. Gloaguen, F.Y. Petillon, P. Schollhammer, J. Talarmin, Inorg. Chem. 49 (2010) 2496–2501.
[21] Z. Wu, M. Wang, P. Li, W. Dong, F. Wang, L. Sun, Dalton Trans. (2008) 2400–2406.
[22] Y. Si, M. Hu, C. Chen, C.R. Chimie 11 (2008) 932–937.
[23] W.-G. Wang, H.-Y. Wang, G. Si, C.-H. Tung, L.-Z. Wu, Dalton Trans. (2009) 2712–2720.
[24] J. Cooke, M. Green, F.G.A. Stone, J. Chem. Soc. A (1968) 170–173.
[25] L. Maresca, F. Greggio, G. Sbrignadello, G. Bor, Inorg. Chim. Acta 5 (1971) 667–674.
[26] E. Kostiner, M.L.N. Reddy, D.S. Urch, A.G. Massey, J. Organomet. Chem. 15 (1968) 383–395.
[27] W. Beck, K.H. Stetter, S. Tadros, K.E. Schwarzhans, Chem. Ber. 100 (1967) 3944–3949.
[28] G.A.N. Felton, B.J. Petro, R.S. Glass, D.L. Lichtenberger, D.H. Evans, J. Am. Chem. Soc. 131 (2009) 11290–11291.
[29] S. Kaur-Ghumaan, L. Schwartz, R. Lomoth, M. Stein, S. Ott, Angew. Chem. Int. Ed. 49 (2010) 8033–8036.
[30] M. Beyler, S. Ezzaher, M. Kornahl, M.-P. Santoni, R. Lomoth, S. Ott, 27 (2011) 11662–11664.